Vibration Spectroscopy Study of Ferroelastoelectric $[(CH_3)_2CHNH_3]_4Cd_3Cl_{10}$ Doped with Copper

V. Kapustianyk[a], Yu. Chornii[a,*], V. Rudyk[b], Z. Czapla[c], R. Cach[c], O. Kolomys[d] and B. Tsykaniuk[d]

[a] *Solid State Physics Chair, Ivan Franko National University of Lviv, Dragomanova str. 50, 79005 Lviv, Ukraine*
[b] *Scientific-Technical and Educational Center of Low-Temperature Studies, Ivan Franko National University of Lviv, Dragomanova str. 50, 79005 Lviv, Ukraine*
[c] *Institute of Experimental Physics, University of Wrocław, pl. M. Borna 9, 50204 Wrocław, Poland*
[d] *V.E. Lashkaryov Institute of Semiconductor Physics NAS of Ukraine, pr. Nauki, 41, 03028 Kyiv, Ukraine*

Received: 13.03.2020 & Accepted: 24.04.2020

Doi: 10.12693/APhysPolA.138.488 *e-mail: ychornii@gmail.com

Infrared absorption spectra of $[(CH_3)_2CHNH_3]_4Cd_2Cl_{10}$:Cu crystals with copper concentration of $0.6 \pm 0.1\%$ and $1.8 \pm 0.1\%$ were investigated in the spectral range of 30–12000 cm^{-1} and Raman spectra of the same crystals were investigated within the range of 30–4000 cm^{-1}. These crystals belong to a large family of compounds with the metal-halogen polyhedra of different types manifesting various phase transitions including those into the ferroelectric, ferroelastic and even ferroelastoelectric phases. The related crystals with an alkylammonium cation and transition metal ions in their structure were found to be multiferroics since they are characterized by the coexistence of ferroelectric and magnetic ordering. The obtained data for $[(CH_3)_2CHNH_3]_4Cd_2Cl_{10}$:Cu crystals were compared with those for the initial compound without copper. Increasing the Cu^{2+} concentration in the crystals leads to merging of bands in the infrared spectra corresponding to the skeletal vibrations of IPA cations because of their interaction with the complex anions consisting of two types of octahedra: $CdCl_6$ and $CuCl_6$. Moreover, for all investigated crystals and geometries of experiment a considerable splitting of the Raman modes corresponding to skeletal vibrations of IPA cation and asymmetric stretching vibrations of the methyl groups were observed. This case corresponds to Davydov's splitting connected with the presence of different numbers of distinct IPA cations. A very similar character and level of the mentioned splitting testifies to the fact that the crystals doped with copper are characterized by the same structure of phase II as the initial IPACC crystal. The doped crystals with a higher concentration of Cu^{2+} manifest very broad bands in the region above 9000 cm^{-1} which would be related to the intra-ion transitions in Cu^{2+} ion. The performed analysis of the IR and Raman spectra both of the initial crystals and those doped with copper allowed to identify more precisely the real phonons which are most of all involved in the formation of the absorption edge.

topics: multiferroics, infrared spectra, Raman spectra, ferroelastoelectric

1. Introduction

The IR and Raman spectra are important sources of information on interactions and molecular dynamics and they are usually used to study phase transitions in newly grown crystals. Such an approach was used for initial crystals of tetra (isopropylammonium) decachlorotricadmate (II) with chemical formula $[(CH_3)_2CHNH_3]_4Cd_3Cl_{10}$ (IPACC) [1]. They are built of a two-dimensional network of Cd_3Cl_{10} units interconnected by isopropylammonium (IPA) cations. These crystals belong to a large family of compounds with the metal-halogen polyhedra of different types manifesting various phase transitions including those into the ferroelectric, ferroelastic and other ferroic phases [2–9]. Some of these crystals were prepared as the nanocomposites and were characterized by the principally new properties. For example, the composites based on the crystals of $[N(C_2H_5)_4]_2CoCl_2Br_2$ were found to possess a clear resonance type dispersion with a frequency in the gigahertz region. The latter depends on the size of individual nanocrystals that is very important for the creation of the principally new piezotransducers [10].

IPACC exhibits several temperature-dependent phase transitions. Dielectric, dilatometric, X-ray, DSC, birefringence and heat capacity studies showed and confirmed three phase transitions

presented in the scheme below (T_1, T_2 and T_3 indicate the phase transition temperatures) [11]:

$$\underset{\text{(I)}}{Cmca} \xrightarrow{T_1 = 353\ \text{K}} \underset{\text{(II)}}{Pbca} \xrightarrow{T_2 = 294\ \text{K}} \underset{\text{(III)}}{P2_12_12_1} \xrightarrow{T_3 = 260\ \text{K}} \underset{\text{(IV)}}{P2_1/b}$$

A partial substitution of the cadmium ion with copper affects the phase transitions in IPACC crystal, chiefly their temperatures since the inorganic anions influence the dynamics of the organic cations which are responsible, at least, for two low temperature phase transitions [12]. Moreover, it is necessary to note that new $[(CH_3)_2CHNH_3]_4Cd_3Cl_{10}$:Cu (IPACCC) compounds — due to doping with Cu^{2+} ions — become of special interest to scientists since they could reveal magnetic properties and possible magnetoelectric coupling. Indeed, the related crystals with an alkylammonium cation and transition metal ions in their structure were found to be multiferroics since they are characterized by the coexistence of ferroelectric and magnetic ordering [13]. On the other hand, the compounds of such a type could also be interesting for nonlinear optics applications [14]. Doping of these crystals with transition metal ions implies the possibility of quite large photoinduced effects, for example, second harmonic generation.

The properties of the doped IPACCC crystals were reported in [12, 15–17]. The EDX analysis showed that the amount of Cu doping did not exceed 0.5%. These crystals will further be denoted as IPACCC (low). It was suggested that the sequence of phases and their structure in IPACCC (low) are very similar to those in the initial crystals and some Cd atoms are statistically replaced with Cu atoms in an anionic complex $[Cd_3Cl_{10}]^{4-}$. This conclusion is confirmed by the data of X-ray diffraction, heat capacity and crystal field spectra study of IPACCC (low) crystals [12]. It was also shown that the temperatures of the corresponding phase transitions in the doped crystals are a little shifted in respect to the initial one [12, 15–17]:

$$\underset{\text{(I)}}{Cmca} \xrightarrow{T_1 = 358\ \text{K}} \underset{\text{(II)}}{Pbca} \xrightarrow{T_2 = 293\ \text{K}} \underset{\text{(III)}}{P2_12_12_1} \xrightarrow{T_3 = 253\ K} \underset{\text{(IV)}}{P2_1/b}$$

Phase III was found to be ferroelastoelectric since the corresponding domain structure was visualized using different modes of atomic force microscopy [17]. The analysis of temperature dependence of the optical birefringence increment showed that the transition into the ferroelastoelectric phase at $T_2 = 293$ K has to be related to the first order, close to the second order [17]. The investigated compounds can be considered a secondary ferroic. Their investigations are of special interest since only a few specific examples of high order ferroics are currently known. This is because they are difficult to identify. Under such circumstances, the IR studies at different temperatures have been undertaken to investigate the molecular interactions' contribution to the phase transition mechanisms. The wavenumbers, relative intensities and proposed assignments of the internal vibrations at 300 K in IPACCC (low) were compared with those in the initial IPACC crystal [16]. These characteristics were obtained for both powder-like compounds in Nujol.

The low temperature phase transitions in IPACCC (low) crystal are known to be due to the change in dynamical states of isopropylammonium cations $[(CH_3)_2CHNH_3]^+$. These changes were found to be reflected in the modifications of positions and shapes of the IR bands corresponding to the internal vibrations of these cations [16].

In this paper we studied the influence of Cu dopant in different concentrations on the vibration spectra and, respectively, the arrangement of structure of the initial IPACC crystal. In this respect, the Raman spectra could be considered a very good complement to the IR spectra. That is why we investigated in a much wider spectral range the IR absorption of single crystal platelets of initial IPACC and doped IPACCC crystals contrary to the case of previous investigations of IPACC and IPACCC (low) performed on the polycrystalline sample in Nujol [1, 16]. The main purpose was further study the dynamics of isopropylammonium cations and the arrangement of the two-dimensional network of the metal-halogen polyhedra of the newly discovered ferroelastoelectrics.

2. Experimental

IPACCC crystal is expected to resemble IPACC in its structure and chemical composition. We compared the vibration spectra of initial IPACC and doped IPACCC crystals with two different concentrations of copper in order to identify their types of vibrations.

Light yellow $[(CH_3)_2CHNH_3]_4Cd_3Cl_{10}$:Cu crystals (IPACCC) were grown at $T = 304$ K from an aqueous solution of $CdCl_2 \cdot 4H_2O$, $CuCl_2$ and $(CH_3)_2NH_2Cl$ salts taken in the stoichiometric ratio with a small excess of HCl. The colorless undoped IPACC crystals were grown in a similar way from an aqueous solution of $CdCl_2 \cdot 4H_2O$ and $(CH_3)_2NH_2Cl$ salts taken in the stoichiometric ratio. Large and good quality samples were obtained after about 4 weeks. All grown crystals exhibited a distinct cleavage plane perpendicular to the b axis.

The Cd to Cu ratio in IPACCC was examined by SEM using a REMMA–102–02 scanning electron microscope. EDX was carried out by using an energy-dispersive X-ray analyzer with pure elements as standards for Ag and Ge, ZnS for S, and KBr for Br (the acceleration voltage was 20 kV and K and L-lines were used).

The Raman measurements were performed in a quasi-backscattering geometry using a confocal JobinYvon T 64000 triple spectrometer equipped with a thermoelectrically cooled silicon charge-coupled device detector. An edge filter was placed in front of the spectrometer entrance to remove

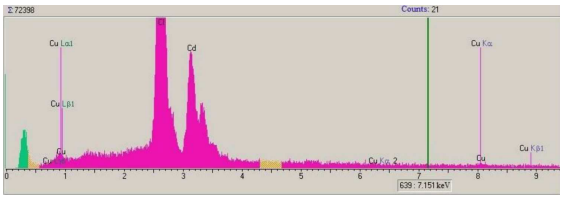

Fig. 1. The EDX analysis data for IPACCC (high) crystals averaged over the surface.

TABLE I

Details of the EDX analysis (for voltage 20 kV).

Element	Int.	C [%]	At. [%]	Coeff.
Cl K	50168	21.73	35.909	69.304
Cu K	254	0.55	0.510	0.984
Cu L	278	0.00	0.000	0.000
Cd L	13495	29.53	15.395	29.712
Total		51.87		100

the elastically dispersed light and an Ar^+ ion laser with line at 488.0 nm was used for excitation. An Olympus BX 41 microscope equipped with a 100× objective (numerical aperture $NA = 0.90$) was used to focus the laser light on the sample to a spot size of ~ 1 μm. The laser power which was directed to the sample surface was always kept below 3 mW in order to obtain an acceptable signal-to-noise ratio and to prevent laser heating. The spectral resolution was about 0.2 cm^{-1}. Correct instrument calibration was verified by checking the position of the emitting line of a Ne lamp at 540.056 nm.

IR transmittance spectra were measured in far- and mid-IR range (30–12000 cm^{-1}) by using a vacuum FTIR Bruker Vertex 70 v spectrometer equipped with Globar source and a deuterated triglycine sulfate (DLaTGS) detector with a polyethylene window. Spectral resolution had the value of 2 cm^{-1} and 64 scans were taken.

Raman and IR spectra were measured at $T = 295$ K. A special cryostat together with a temperature controller UTREX and a germanium temperature sensor provided the necessary stabilization and precision of the temperature measurements ($\Delta T = \pm 0.1$ K).

3. Results and discussion

The EDX analysis showed that the amount of Cu doping did not exceed $0.6 \pm 0.1\%$ for IPACCC (low) [15] and $1.8 \pm 0.1\%$ for IPACCC (high) (see Fig. 1). The pronounced yellowish color of the samples clearly indicates that Cu^{2+} ions are implemented into the crystal structure. Interesting detailes can be also found in Table I.

3.1. IR spectra

The IR spectra of IPACC and IPACCC crystals with different concentrations of a Cu^{2+} ion are shown in Figs. 2–4. Most of the vibration

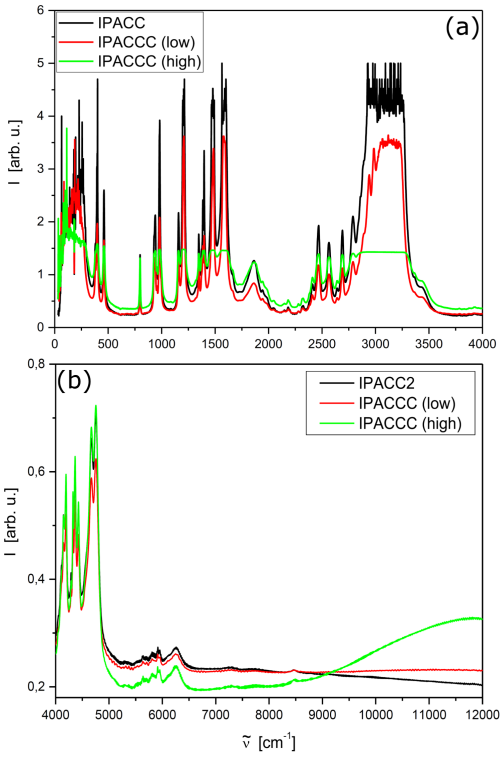

Fig. 2. Comparison of the infrared absorption spectra of initial IPACC and doped IPACCC crystals.

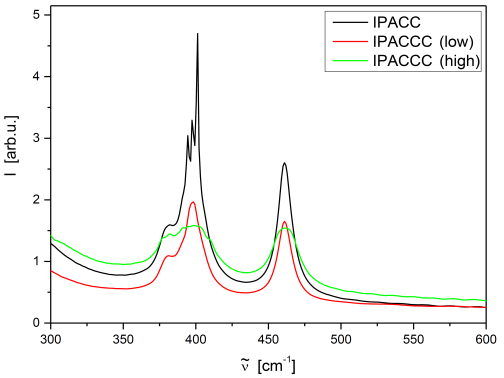

Fig. 3. Infrared absorption spectra of IPACC and IPACCC crystals at the range 300–600 cm^{-1}.

modes for all compared crystals coincide in frequency. This means that all considered crystals are isostructural and Cu^{2+} ion statistically replaces Cd^{2+} ions in the anion complex. Under such circumstances, we can apply a factor-group analysis performed for the initial crystals [1] also to the anion complex in IPACCC (Table II). According to [1, 16], the latter consists of three metal-halogen octahedra of two types.

The wavenumbers of the vibration modes can be easily identified by comparison with the data obtained in [16] for the samples of IPACC and IPACCC (low). Nevertheless, it is necessary to bear in mind that these investigations were performed on polycrystals in Nujol. It is also important to note

TABLE II

Classification of the fundamental modes for IPACC and IPACCC (low) crystals for phase II. Abbreviations: A_c — acoustic modes, T — translational type lattice modes, L — librational type lattice modes, I — inactive, Me — metal.

	A_c	Lattice modes				Internal modes			Selection rules	
		IPA		$[Me_3Cl_{10}]^{4-}$		IPA1	IPA2	$[Me_3Cl_{10}]^{4-}$	IR	Raman
		L	T	L	T					
A_g		6	6		3	36	36	15	I	xx, yy, zz
B_{1g}		6	6		3	36	36	15	I	Xy
B_{2g}		6	6		3	36	36	15	I	Zx
B_{3g}		6	6		3	36	36	15	I	Yz
A_u		6	6	3		36	36	18	I	I
B_{1u}	1	6	6	2		36	36	18	Z	I
B_{2u}	1	6	6	2		36	36	18	Y	I
B_{3u}	1	6	6	2		36	36	18	X	I

that in this paper we investigated single crystals' platelets. That is why strong bands in the vicinity of 2800–3300 cm^{-1} are hardly distinguished even for very thin samples ($\sim$ 0.1 mm). This particularly concerns IPACCC with higher copper concentration. This spectral region corresponds to the vibrations of CH_3 and NH_3 group and the overtones of other modes. Fortunately, these bands were identified for IPACC [1] and IPACCC (low) [16] powder in Nujol. We hardly expect any considerable changes of these modes for the single crystals doped with copper. But such a problem was observed only for these bands. The other bands were less intensive and clearly distinguished. They possess a characteristic shape for the vibrational modes and were analyzed without problems. The new features observed in the mentioned frequency range for the doped crystals, particularly for the newly grown IPACCC (high) compound, will be discussed later.

The IR absorption spectra at the higher wavenumber region were observed for the first time for all investigated crystals (see Fig. 2b). Positions of these absorption bands in the range of 4000–6500 cm^{-1} practically coincide for all compared crystals. They also would be related to the overtones of the modes corresponding to the methyl group and ammonium head vibrations. Such a behavior confirms the similarity in the arrangement of the organic subsystem in the three investigated compounds.

A much more pronounced difference was found to appear at the spectral range above 9000 cm^{-1}. The absorption coefficient in this region grows considerably with increasing copper ions' concentration. The corresponding absorption in both IPACCC crystals is connected with the internal electron transitions in the copper ion in the copper-halogen polyhedra. The corresponding crystal field spectra were analyzed in detail for IPACCC with lower copper concentration [12]. The presence of similar bands of considerably higher intensity in IPACCC (high) looks natural. This allows to conclude that

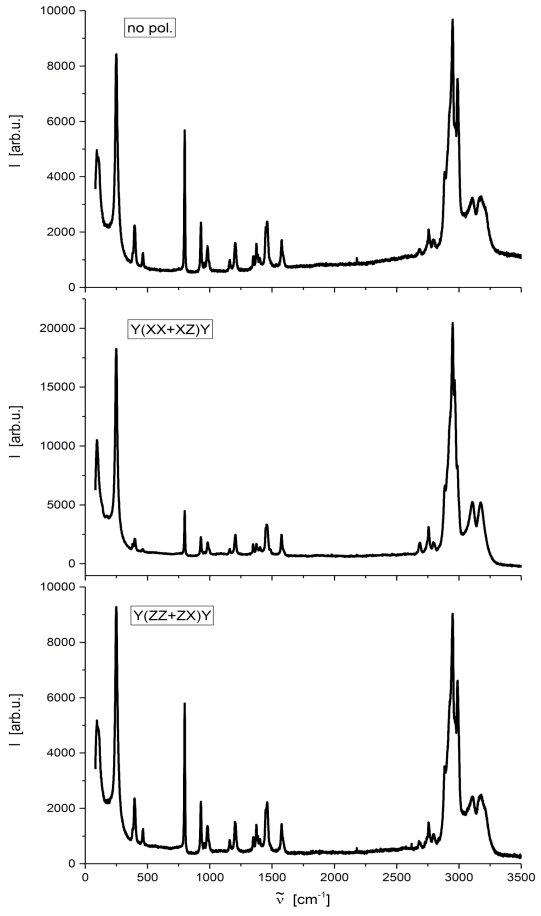

Fig. 4. Raman spectra of IPACCC (low) crystal at different geometries of experiment.

the structure of IPACCC (high) is similar to those of IPACCC (low), as well as to those of the initial crystal without a copper addition. The anionic complex was found to possess a similar symmetry in all three compounds and consists of the three metal-halogen octahedra of two types with different orientation of their axes relatively to the main crystallographic directions.

Although for the majority of the modes observed in the IR spectra of all three investigated crystals we could accept the identification presented in [1, 16] for IPACC and IPACCC (low), it would also be interesting to consider new specific features appearing in the low frequency part of the IR spectra due to the doping of the initial crystal with copper.

Figure 3 presents the infrared absorption spectra of IPACC and IPACCC in the range of 300–600 cm^{-1}. The modes located at 379, 399 and 460 cm^{-1} are clearly observed in the obtained spectra. They are related to δ_s (CCC) and δ_s (CCN) vibration types. These are the deformation modes of the organic "skeleton". In IPACC crystal, the band in the vicinity of 400 cm^{-1} splits onto three closely spaced narrow bands at 394, 397 and 401 cm^{-1}. Isomorphic substitution results in the merging of these three bands into a single, substantially wider band in IPACCC. Such a substitution of a metal ion is accompanied by the appearance of the octahedra of two types, namely $CdCl_6$ and $CuCl_6$, which are statistically distributed in complex anions. The revealed effect is the evidence of indirect influence of isomorphic substitution of metal ions on the internal vibrations and ordering processes in the organic subsystem of the studied crystals.

3.2. Raman spectra

On the basis of the polarized Raman spectra analysis detailed information may be obtained about the symmetry of the vibration modes and, respectively, about the peculiarities of a certain structural group arrangement. On the other hand, we used a Raman microscope in our investigations and the choice of possible variants of the scattering geometry was limited. The second restriction was connected with a layered character of the crystal structure arrangement. Taking into account these conditions, we analyzed Raman scattering at the so-called 180° geometry when a sample is irradiated with a polarized light along Y axis and the scattered light is analyzed in the same direction.

Table II shows vibrations of the $A_g(xx, yy, zz)$, $B_{1g}(xy)$, $B_{2g}(xz)$ and $B_{3g}(yz)$ types that have to be active in the Raman spectra. Figure 4 presents the nonpolarized and polarized Raman spectra of IPACCC (low) crystal obtained in the following geometries: $Y(ZZ + XZ)Y$ and $Y(XX + ZX)Y$. The nonpolarized spectrum would be considered as a sum of the two spectra mentioned above. The assignments of the bands collected in Table III have been based on acomparison with the vibration spectra of IPACC [1], IPACCC (low) [16], isopropylammonium cations [18–20] and an isopropylamine molecule [21].The vibrations of B_{2g} type and corresponding bands at 93, 248, 1456, 2756, 2949, 3106, 3173 cm^{-1} are active in $Y(XX + XZ)Y$ geometry. The intensity of these bands is much higher than those for the corresponding bands observed in $Y(ZZ + ZX)Y$ geometry and

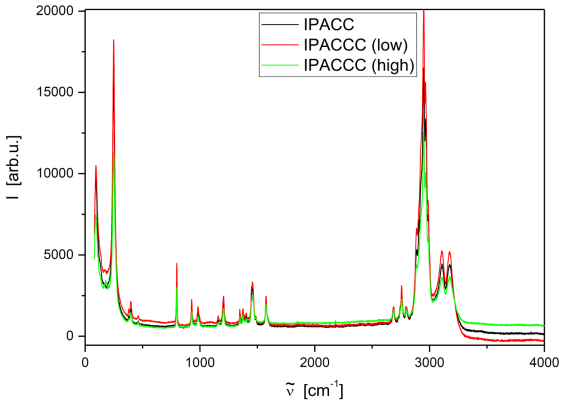

Fig. 5. Raman spectra of IPACC and IPACCC crystals with different concentrations of copper analyzed without a polarizer in the range of 0–4000 cm^{-1}.

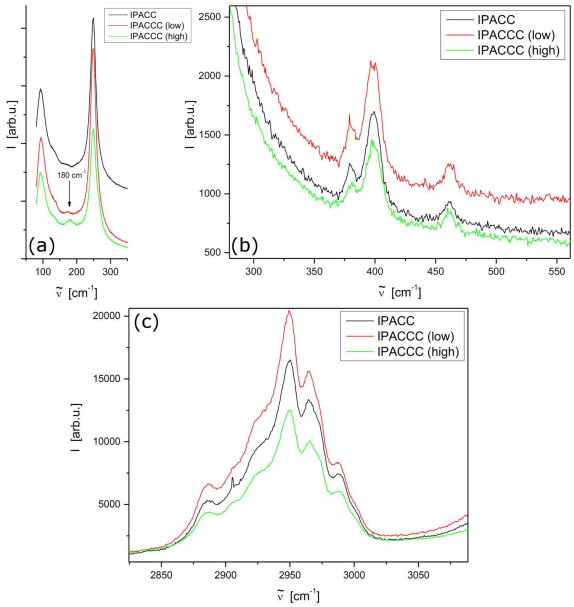

Fig. 6. Raman spectra of IPACC and IPACCC crystals with different concentrations of copper in the range of 80–570 cm^{-1} (the spectra are shown in the same scale but shifted along the ordinate axis).

in the nonpolarized spectra. On the other hand, the band at 798 cm^{-1} at polarization geometry $Y(ZZ + ZX)Y$ possesses a considerably higher intensity than those for $Y(XX + XZ)Y$.

Contrary to the case of IR spectra, in $Y(ZZ + ZX)Y$ geometry there are two bands corresponding to δ_s(CCC) skeletal vibrations at 382 and 396 cm^{-1}, whereas for $Y(XX + XZ)Y$ geometry the splitting into the three ones at 379 cm^{-1}, 396 cm^{-1} and 400 cm^{-1} was observed. They should be attributed also to vibrations of B_{2g} type. This case corresponds to Davydov's splitting. It would also be interesting to compare the Raman spectra for the crystals with different copper concentration (Figs. 5 and 6).

TABLE III

Experimental frequencies [cm^{-1}] on single data, relative intensities and tentative assignments of the bands observed in the Raman spectra of IPACC and IPACCC crystals with different concentration of copper: vs — very strong, s — strong, m — medium, w — weak, vw — very weak, sh — shoulder.

IPACCC				IPACC	Tentative assignment
$Y(XX+XZ)Y$	$Y(ZZ+ZX)Y$	Nonpolarised		Nonpolarised	
Low	Low	High	Low		
93 s	93 s	92 s	93 s	93 s	ν_5(Cd–Cl)
			139 w	136 w	ν_2(Cd–Cl)
171 vw	183 vw	181 vw	173 vw		ν_2(Cu–Cl)
248vs	248 vs	248 vs	249 vs	249 vs	ν_1(Cd–Cl)
379 vw	382 vw	381 vw	379 vw	379 vw	δ_s(CCC), δ_s(CCN)
396 w, 400 w	396 w	398 w, 401 w	396 w, 400 w	399 w	δ_s(CCC)
461 vw	463 vw	459 vw	460 vw	461 vw	δ(CCN)
798 m	798 m	798 m	798 m	799 m	v_s(CCC)
927 w	928 w	929 w	929 w	928 w	ν_a(CCN)
958 vw	958 vw				$\rho(CH_3)$
983 w	981 w	983 w	984 w	983 w	v(CN)
1158 vw	1159 vw	1157 vw	1158 vw	1159 vw	v_a(CCC)
1205 w	1203 w	1204 w	1206 w	1206 w	$\tau(NH_3^+)$
1347 vw	1350 vw	1347 vw	1345 vw	1346 vw	δ(CH)
1375 vw	1373 vw	1374 vw	1374 vw	1374 vw	$\delta_s(CH_3)$
1385 vw		1385 vw	1385 vw	1386 vw	$\delta_s(CH_3)$
1404 vw	1404 vw	1403 vw	1403 vw	1403 vw	$\delta(CH_3)$
1456 w	1456 w	1449 w	1449 w	1449 w	$\delta_a(CH_3)$
1576 w	1575 w	1575 w	1576 w	1576 w	$\delta_a(NH_3^+)$
2685 w	2686 vw	2687 vw	2685 vw	2685 vw	N–H, C–H
2756 w	2755 w	2748 w	2755 w	2756 w	N–H, C–H
2794 vw	2792 vw	2795 vw	2794 vw	2796 vw	N–H, C–H
2885 vw	2885vw	2887 vw	2886 vw	2885 vw	$v_s(CH_3)$
2905 sh, 2923 sh, 2949 vs, 2965 sh	2904 sh, 2922 sh, 2949 vs, 2965 sh	2906 sh, 2922 sh, 2949 vs, 2965 sh	2904 sh, 2922 sh, 2949 vs, 2965 sh	2903 sh, 2924 sh, 2949 vs, 2965 sh	$v_a(CH_3)$
2987 s	2988 s	2988 s	2981 s	2988 s	$v_a(CH_3)$
3106 m	3109 m	3105 m	3108 m	3110 m	$v_s(NH_3^+)$
3174 m	3177 m	3172 m	3172 m	3173 m	$v_a(NH_3^+)$

It is necessary to note that a similar splitting is also characteristic for IPACCC (high): 381 cm^{-1}, 398 cm^{-1}, 400 cm^{-1}, whereas the initial crystal is characterized by two components at 379 cm^{-1} and 399 cm^{-1}. Basing on the factor-group analysis (Table II) and analysis performed for the initial crystal [1], it could be concluded that in phase II for all considered compounds there are two symmetry independent IPA cations which occupy the C_1 (8) sites and are still disordered. All isopropylammonium internal modes ($36A$) are IR and Raman active and may split into $A_u + A_g$, under the assumption that the coupling between the internal vibrations of IPA cations is related in one formal molecule by C_i symmetry. The Davydov type interaction between the four symmetry equivalent molecules in a primitive unit cell leads to further splitting: $A_g \to A_g + B_{1g} + B_{2g} + B_{3g}$ and $A_u \to A_u + B_u + B_{2u} + B_{3u}$ [1].

Furthermore, for all investigated crystals and geometries of experiment there was observed a considerable splitting of $v_a(CH_3)$ band at 2949 cm^{-1} into four or five bands that would also be related to Davydov's splitting. Such a behaviour reflects the specific arrangement of the organic subsystem in phase II. It means that changes in the dynamical state of the cation are noticeable. These conclusions correlate with the data of an X-ray diffraction study for the initial IPACC crystal [11]. It is known that in phase II four groups of cations

TABLE IV

Correlation between the vibration modes and the effective energies of phonons participating in the formation of the absorption edge calculated on the basis of the Urbach's rule analysis (the effective energies are presented in cm^{-1} for convenience)

Crystal (type of the absorption edge) polarization	T [K]	$\tilde{\nu}_0$ [cm^{-1}]	IPACC		IPACCC (low)		Identification of vibrational modes
			IR	Raman	IR	Raman	
IPACC	255–294	485	460 m	461			δ(CCN)
(fundamental) $\boldsymbol{E}\|\|a$	294–353	155		136 sh			ν_2Cd–Cl
IPACCC (low)	255–293	157			149 vs	139 sh	ν_2Cd–Cl
(fundamental) $\boldsymbol{E}\|\|a$						173 vw	ν_2Cu–Cl
IPACCC (low)	255–293	335			325 vw		ν_3Cu–Cl
(fundamental) $\boldsymbol{E}\|\|c$	293–355	75			76		trans CCN
IPACCC (low)	255–295	267			247 m	249 s	ν_1Cu–Cl
(CT) $\boldsymbol{E}\|\|a$	293–355	338			325 vw		ν_3Cu–Cl

are arranged, namely IPA-A, IPA-B, IPA-C and IPA-D [11]. All the IPA cations in this phase were found to be still disordered. IPA-A from the parent phase I is disordered over two IPA-A and IPA-D positions with 0.5 occupancy, whereas IPA-B is distributed over IPA-B and IPA-C with 0.45 (1) and 0.55 (1) occupancy.

The situation in the ferroelastoelectric phase III is expected to be very similar in respect to Davydov's splitting of the modes corresponding to vibrations within IPA cations. According to [11], transformation from phase II to III is induced by the ordering of IPA cations. IPA-A and IPA-D are still disordered and adopt two nonequivalent positions in the crystal structure with 50% probability (IPA-A1, IPA-A2 and IPA-D1, IPA-D2). In principle, the presence of different numbers of distinct IPA cations, depending on the particular phase, leads to a different degree of Davydov's splitting of the bands associated with the internal vibrations of these cations. This alteration shows that not only the skeletal vibrations or CH_3 and NH_3 modes but also the corresponding overtones are sensitive to the ordering of the organic cations. Taking into account a very similar character and level of the above mentioned splitting it could be supposed that the crystals doped with copper would be characterized by the same nature of the phase transitions between phases I, II and III as the initial IPACC crystal.

Raman spectra of IPACC and IPACCC crystals with high and low Cu^{2+} concentration in the range of 50–350 cm^{-1} are compared in Fig. 6a. The weak bands around 180 cm^{-1} (173 cm^{-1} for a lower concentration of copper) are noticeable in the Raman spectrum of IPACCC crystals. Taking into account that this mode is hardly seen in the spectrum of the initial crystal, it could be attributed to the internal valence vibration of ν_2(Cu–Cl) type in the octahedron. Such a conclusion fairly well correlates with the data of [22] where a corresponding well-pronounced band was observed in the Raman spectra of $[(CH_3)_2NH_2]_5Cd_2CuCl_{11}$ crystal within the range of 176–184 cm^{-1} depending on the geometry of experiment. It is necessary to note that this compound is characterized by an arrangement of the complex metal-halogen polyhedron very similar to those in the investigated IPACCC. On the other hand, such an assignment looks natural since ν_2(Cu–Cl) mode is shifted toward the higher values of the wavenumbers in respect to ν_2(Cd–Cl) due to a lower mass of copper ion as compared with cadmium. The presence of these modes in the spectrum of IPACCC crystals together with the data of IR spectroscopy in the region of high wavenumbers confirms that Cu^{2+} ion statistically replaces Cd^{2+} ion in the metal-halogen octahedra. At the same time, the very low intensity of this mode testifies to the fact that we do not observe any pronounced resonance Raman scattering.

3.3. Formation of the absorption edge

The performed identification of the vibration modes for the investigated crystals could be very useful for a more precise analysis of the electron-phonon interaction responsible for the formation of their absorption edge. The previously performed spectral investigations ascertained a noticeable influence of the doping with Cu^{2+} ions on the electron-phonon interaction and respectively on the shape and temperature evolution of the optical absorption edge of IPACC and IPACCC (low) crystals [15].Due to this interaction, for phases II and III of both IPACC and IPACCC crystals the low energy tails of the absorption edge bands are described by the empirical Urbach's rule. The values of effective energy $\hbar\omega_0$ of phonons participating in the formation of the absorption edge were calculated for different phases of both crystals [15]. It would be convenient to compare them with the energies of

certain vibration modes obtained by means of vibration spectroscopy. Unfortunately, the set of the corresponding data was incomplete by the end of our investigations.

The real phonons predominantly involved in the formation of the absorption edge might be more precisely identified and their exact position in the spectrum might be determined only after the analysis of the IR and Raman spectra both of the initial crystals and crystals doped with copper, including those presented in [16]. These effective values of the phonons participating in the EPI (Table IV) were found to be very close to the energies (wavenumbers) of the real internal vibrations of the metal-halogen octahedra and skeletal (or translational) vibrations of IPA cation.

It has been found that the low energy tail of the charge transfer (CT) band in phases II and III of IPACCC is formed with participation of the internal vibrations of the copper-halogen polyhedron. This looks natural since the process of charge transfer proceeds exactly within this complex. The tail of the fundamental absorption edge for IPACCC is formed with participation of the internal vibrations of the metal-halogen complex in the ferroelastoelectric phase III and translational vibration of IPA cation in phase II ($\boldsymbol{E}||c$). On the other hand, the skeletal vibrations of the organic group (C–C–N) are most of all responsible for the formation of the absorption edge in phase III, whereas the internal vibrations of the metal-halogen complex participate in this process in phase II of IPACC. In this analysis, we assumed that the energies of the above mentioned modes practically do not depend on temperature which is confirmed by the investigations of the temperature evolution of the infrared absorption spectra of IPACC [1] and IPACCC (low) [16].

4. Conclusions

Infrared absorption spectra and Raman spectra of $[(CH_3)_2CHNH_3]_4Cd_2Cl_{10}$:Cu crystals with different concentration of copper were investigated in a wide spectrum range. On the basis of the comparative analysis of these data and those for the undoped crystal, it has been found that all considered compounds possess a very similar structure. In all cases the anionic complex has the same symmetry and consists of the three distorted metal-halogen octahedra with different orientation of their axes in respect to the main crystallographic directions. Cu^{2+} ion in these octahedra statistically replaces Cd^{2+}. Increasing of Cu^{2+} concentration in the crystals leads to merging of bands in the infrared spectra corresponding to the skeletal vibrations of IPA cations because of their interaction with the complex anions octahedra of two types — $CdCl_6$ and $CuCl_6$. At the same time, the doped crystals with a higher concentration of Cu^{2+} manifest very broad bands in the region above 9000 cm^{-1}, that would be referred to the intra-ion transitions in Cu^{2+} ion. On the other hand, a weak band around 181 cm^{-1} arises in the Raman spectra of the doped crystals being the most pronounced in the samples with a higher concentration of Cu^{2+}. This band corresponds to the internal valence vibration of ν_2(Cu–Cl) type in the octahedron.

Furthermore, for all investigated crystals and geometries of experiment there was observed a considerable splitting of the Raman modes corresponding to the skeletal vibrations of IPA cation and asymmetric stretching vibrations of the methyl groups. This case corresponds to Davydov's splitting connected with the presence of different numbers of distinct IPA cations. According to [1], phases II and III (ferroelastoelectric) are characterized by four groups of different IPA cations. Taking into account a very similar character and level of the mentioned splitting, it could be supposed that the crystals doped with copper would be characterized by the same nature of the phase transitions between phases I, II and III as the initial IPACC crystal.

The performed analysis of the IR and Raman spectra both of the initial crystals and crystals doped with copper, including those presented in [1, 16], allowed to identify more precisely the real phonons predominantly involved into the formation of the absorption edge and to determine their exact position in the spectrum. The effective values of the energies of phonons participating in the EPI were found to be very close to the energies (wavenumbers) of the real internal vibrations of the metal-halogen octahedra and skeletal (or translational) vibrations of IPA cation.

References

[1] B. Staskiewicz, J. Baran, Z. Czapla, *J. Phys. Chem. Solids* **74**, 1848 (2013).

[2] V. Kapustianyk, V. Rudyk, M. Partyka, *Phys. Status Solidi (b)* **244**, 2151 (2007).

[3] V.B. Kapustianik, I.I. Polovinko, S.A. Sveleba, O.G. Vlokh, Z.A. Bobrova, V.M. Varikash, *Phys. Status Solidi (a)* **133**, 45 (1992).

[4] V.B. Kapustianik, V.V. Bazhan, Yu.M. Korchak, *Phys. Status Solidi (b)* **234**, 674 (2002).

[5] W.-Q. Liao, G.-Q. Mei, H.-Y. Ye, Y.-X. Mei, Y. Zhang, *Inorg. Chem.* **53**, 8913 (2014).

[6] G.-Q. Mei, W.-Q. Liao, *J. Mater. Chem. C* **33**, 8535 (2015).

[7] Y. Lu, Z. Wang, H.P. Chen, J.-Z. Ge, *Cryst. Eng. Comm.* **19**, 1896 (2017).

[8] Q. Ji, L. Li, S. Deng, X. Cao, L. Chen, *Dalton Trans.* **47**, 5630 (2018).

[9] M.S. Lassoued, A. lassoued, M.S.M. Abdelbaky, S. Ammar, A. Ben Salah, A. Gadri, S. Garcia-Granda, *J. Mol. Struct.* **1165**, 42 (2018).

[10] V. Kapustianyk, Ya. Shchur, I. Kityk, V. Rudyk, G. Lach, L. Laskowski, S. Tkaczyk, J. Swiatek, V. Davydov, *J. Phys. Condens. Matter* **20**, 365215 (2008).

[11] A. Gagor, A. Waskowska, Z. Czapla, S. Dacko, *Acta Cryst (b)* **67**, 122 (2011).

[12] V. Kapustianyk, P. Yonak, V. Rudyk, Z. Czapla, D. Podsiadla, Yu. Eliyashevskyy, A. Kozdraś, P. Demchenko, R. Serkiz, *J. Phys. Chem. Solids* **121**, 210 (2018).

[13] B. Kundys, A. Lappas, M. Viret, V. Kapustianyk, V. Rudyk, S. Semak, Ch. Simon, I. Bakaimi, *Phys. Rev. B* **81**, 224434 (2010).

[14] V. Rudyk, I. Kityk, V. Kapustianyk, K. Ozga, *Ferroelectrics* **330**, 19 (2006).

[15] V. Kapustianyk, P. Yonak, V. Rudyk, Z. Czapla, R. Cach., *Acta Phys. Pol. A* **136**, 208 (2019).

[16] V. Kapustianyk, Yu. Chornii, Z. Czapla, O. Czupinski, *J. Phys. Stud.* (2020); to be published.

[17] V. Kapustianyk, Z. Czapla, V. Rudyk, Yu. Eliyashevskyy, P. Yonak, S. Sveleba, *Ferroelectrics* **540**, 212 (2019).

[18] R. Jakubas, G. Bator, P. Ciąpała, J. Zaleski, J. Baran, J. Lefebvre, *J. Phys. Condens. Matter* **7**, 5335 (1995).

[19] M. Hamada, *Chem. Phys.* **125**, 55 (1988).

[20] I. Chaabane, F. Hlel, K. Guidara, *PMC Phys. B* **1**, 11 (2008).

[21] D. Zeroka, J.O. Jensen, A.C. Samuels, *Int. J. Quantum Chem.* **72**, 109 (1999).

[22] V. Kapustianyk, A. Batiuk, Z. Czapla, D. Podsiadła, O. Czupinski, Yu. Eliyachevskyy, V. Rudyk, *Phys. Stat. Sol. (b)* **241**, 2620 (2004).